Available online at www.sciencedirect.com

ScienceDirect

Ceramics International 40 (2014) 4777–4784

CERAMICS INTERNATIONAL

www.elsevier.com/locate/ceramint

Sago starch as binder and pore-forming agent for the fabrication of porcelain foam

Abdul Rashid Jamaludin[a], Shah Rizal Kasim[a], Mohd Zukifly Abdullah[b], Zainal Arifin Ahmad[a,*]

[a]*Structural Materials Niche Area, School of Materials and Mineral Resources, Engineering Campus, Universiti Sains Malaysia, 14300 Nibong Tebal, Penang, Malaysia*

[b]*Porous Media Combustion Laboratory, School of Mechanical Engineering, Engineering Campus, Universiti Sains Malaysia, 14300 Nibong Tebal, Penang, Malaysia*

Received 18 July 2013; received in revised form 3 September 2013; accepted 7 September 2013
Available online 20 September 2013

Abstract

The aim of this study is to verify the potential of sago starch (*Metroxylon sagu*) as a binder and pore-forming agent for the fabrication of porcelain foam. The porcelain foam was fabricated via the polymeric foam replication technique. Initially, the porcelain raw material was mixed in water with several binders (respectively) to form a slurry. Replication starts by fully submerging a compressed sponge in the slurry. Excess slurry was then removed by hand squeezed and pressed between two parallel plates. Subsequently, the impregnated sponge was sintered at 500 °C and up to 1250 °C for 2 h for sponge and binder removal and porcelain to mature, respectively. The results from this work showed that sago starch slurry produced porcelain with density, total porosity and compressive strength of 0.37–0.51 g cm^{-3}, 79–81%, and 0.33–0.93 MPa, respectively. The increased of porosity and compressive strength are perhaps due to the addition of sago starch which changed the rheological property of the slurry from Newtonian to pseudoplastic behavior. This results in higher value of viscosity, consequently allowing the construction of smoother and uniform cell skeleton although with existence of micro-pores on the structure, which contributed to higher compressive strength. The results from this study showed that sago starch has huge potential as a binder and a pore-forming agent, whilst providing a simpler and cheaper route for the fabrication of cellular ceramics.

Keywords: A. Sintering; B. Porosity; D. Porcelain; Sago starch

1. Introduction

Cellular ceramics materials are used in many fields due to the unique structure. Cellular ceramic poses combination of properties such as low density, high porosity, low thermal conductivity, high permeability, high specific surface area, and high temperature resistance. Some of the applications include porous ceramic material as inorganic membrane reactor [1], porous medium burner (PMB) for gas and liquid combustion [2], thermal barrier [3], ceramic–metal composite preform [4], and also electrical power generation through thermo-photovoltaic system [5]. Cellular ceramics can be produced from different types of materials such as low cost kaolin [6] and porcelain [7,8], alumina [9], mullite [10], silicon carbide (SiC) [11], and zirconia-based ceramics [12].

The quality and properties of the cellular ceramics are dependent on the cell size, size distribution and interconnection, strength and stiffness of the wall or strut. These requirements are strictly dependent on the production processing route, and the intended application. Therefore, many different methods for the production of cellular ceramics have been developed, such as the replication technique [7,13,14], gel-casting [15], freeze casting [16], extrusion [17], compaction [18], and starch consolidation casting (SCC) [9].

However, the most popular production method is the polymeric foam replication technique using highly porous polymer foam (typically polyurethane (PU)) as the template material with varied cell size. The template is impregnated into a ceramic slurry until the internal cells are filled and is

*Corresponding author. Tel.: +60 45996128; fax: +60 459 41011.
E-mail address: zainal@eng.usm.my (Z.A. Ahmad).

0272-8842/$ - see front matter © 2013 Elsevier Ltd and Techna Group S.r.l. All rights reserved.
http://dx.doi.org/10.1016/j.ceramint.2013.09.023

followed by several squeezing steps to remove any excess slurry and to enable the formation of ceramic coating. The removal of the template happened during the sintering process, exhibiting open and closed cells morphology inherited from the original template. The replication technique has several advantages in terms of the reproducibility and suitability of the foam to retain its shape during fabrication process. Besides that, it also shows limited tolerance of cell size and size distribution, moreover the template is completely burnt during sintering. Microscopic flaws tend to occur on the sintered skeleton structure due to the stress developed during the sintering process due to gas evolution from the pyrolysis of the polymer template. Moreover, the triangular void left by the burnt polymer at the interconnections of the skeletons tend to produces high stress concentration at the skeleton corner thus weakening the structure, especially if the slurry coating is thin. This affects the mechanical properties of the structure. Nevertheless, the presence of voids in the skeletons after sintering generally does not reduce the properties but gives benefit in term of better property to mass ratios [19].

Porcelain that can tolerate temperatures of up to 1300 °C was chosen for this study. It is abundant, low cost, non-toxic, easy to handle and store, and not reactive in the presence of water. The slurry used for sponge impregnation is a mixture of ceramic powder and various additives which act as pore-forming agents and binders to facilitate the coating process and adherence of the slurry to the template. Binders typically consist of long chains of polymer networks that serve the primary function of providing strength to the green body by building bridges between particles. In some cases, it also provides plasticity and assists the body forming process [18]. The binders will subsequently eliminated during sintering process, leaving pores on the skeleton or cell wall. These binders, in the form of starch from plants (i.e., tubers or roots and cereal), are the primary sources of environmentally-friendly material (defect-free burnout at low temperature), easy to handle and process, low cost and consistent, have well-rounded shape and size distribution, biodegradable, and readily available biopolymers consisting of condensed glucose units (amylose and amylopectin) [20,21]. In the presence of excess water at moderately elevated temperatures, starch will undergo a process of irreversible swelling and crystalline melting called gelatinization caused by the partial dissolution or collapse (disruption) of molecular order of the starch glucose unit and is transformed from a purely viscous suspension to visco-elastic gel [12].

The types of binder used for the fabrication of porous ceramic are various, including potato, corn, tapioca, rice, wheat, and poppy seed [21–24]. However, currently there is no literature regarding the use of sago (*Metroxylon sagu*), a source of starch used as a binder for the production of cellular ceramic. Sago starch possesses similar properties as the previously mentioned binders but it is somewhat neglected and given relatively less attention despite it being native to Malaysia, abundant, cheap and its repute as a component used in the production of adhesive. Sago starch is easy to gelatinise because of its low gelatinisation temperature, has high viscosity and low gel syneresis as well as being easy to shape [25,26]. The utilization of conventional starch usually results in cellular ceramics with high porosity but low strength. Therefore, this paper presents a comparison of commercially available tapioca starch with sago starch and the possibility of using sago as a highly potential binder and pore-forming agent for fabrication of cellular ceramic in the near future.

2. Experimental

Ready-made porcelain raw powder (Ipoh Ceramic Sdn Bhd) and two different binders i.e., tapioca (mean particle size is 13.85 μm) and sago starch (mean particle size is 94.43 μm) were used for the preparation of slurries. The solid content was varied at 50, 60, and 70 wt% and the binder was fixed at 5 wt %. Distilled water added with 0.5 wt% sodium silicate (Na_2SiO_4); a type of dispersing agent was used as the mixing medium. The solution was heated to 65–70 °C prior to the addition of binders before the mixing process was done. A batch without the addition of binder was prepared as the reference sample. All compositions (Table 1) were mixed for 24 h using polyethylene bottle.

A commercial PU sponge (CCT Automation Sdn Bhd) with interconnected and average cell size of ~16 pores per cm (ppcm) was chosen as the template, and cut into smaller dimensions (100 mm × 100 mm × 25 mm). During the replication process, the sponge was fully submerged while being compressed in the porcelain slurry in order to fill in the template and purge all the trapped air. Subsequently, the impregnated sponge was taken out, squeezed manually by hand and pressed between two parallel plates with a constant gap. These actions were repeated for a couple of times to ensure adequate filling of slurry, remove excess slurry as well

Table 1
Batch composition used in the experiment.

Binder system	Code	Weight percent (wt%)			
		Porcelain raw material	Distilled water	Binder	Dispersant agent
Without binder (reference)	P.5:5	50	50	0	0.5
	P.6:4	60	40	0	0.5
	P.7:3	70	30	0	0.5
Tapioca	P.5:5. T5	50	50	5	0.5
	P.6:4. T5	60	40	5	0.5
	P.7:3. T5	70	30	5	0.5
Sago	P.5:5. SG5	50	50	5	0.5
	P.6:4. SG5	60	40	5	0.5
	P.7:3. SG5	70	30	5	0.5

P: porcelain; T: tapioca; and SG: sago

as to achieve a well-distributed coating. The sample was dried at room temperature for 48 h before being put in an oven for 24 h at 80 °C. The dried sponges were sintered in air using an electrical furnace (Ceramtech 1700) according to the following schedule: the starting heating rate was 5 °C/min up to 500 °C (soak for 1 h) and then further heating up to 1250 °C (hold for 2 h) before cooling down to room temperature.

The particle size distributions of binders were determined using the Mastersizer S (Malvern Instrument Ltd., UK). A thermal gravimetric analysis (TGA) (STARe System Mettler Toledo, Switzerland) was carried out on the binders and sponge, samples between 15 and 20 mg were placed onto a pan and heated at a rate of 10 °C/min from room to an elevated temperature. The viscosities of the slurries were measured using the Polyvisc, Viscostar H viscometer (spindle R3) at different shear rates. The micro-structural morphology of the cell skeleton, and pores were established using the table top scanning electron microscopy (SEM TM3000 Hitachi, Japan) and the phase analysis of the sintered samples was done via the X-ray diffraction method (XRD Bruker D8 Advance, Germany) with CuKα monochromatic radiation ($\lambda = 1.5406$ Å). The diffraction angle 2-theta was adjusted from 10° to 90° with other operating condition are as follows: step interval 0.034° and step time 71.6 s. Archimedes water displacement technique was used to measure the bulk density and total porosity of the sintered samples based on the following formulas:

$$\rho_b = \frac{m_1}{m_3 - m_2} \times 1.0 \text{ g cm}^{-3} \quad (1)$$

$$P_o = \frac{m_3 - m_2}{m_3 - m_1} \times 100\% \quad (2)$$

$$P = 1 - \frac{\rho_b}{\rho_{th}} \times 100\% \quad (3)$$

where ρ_b and ρ_{th} represent the bulk and theoretical density of sintered porcelain foam, whilst P_o and P are the open porosity and total porosity, respectively. ρ_b is calculated using water ($\rho_{water} = 1$ g cm^{-3}) as the medium for relative comparison and ρ_{th} is attained from the density test measured with a gas pycnometer (Micromeritics AccuPyc 1330). m_1 is the dried weight of the sample, whereas m_2 and m_3 are the weight of the sample measured after immersed in water placed in a vacuum container and in air after water saturated, respectively.

The compressive strength was measured for sintered samples using an universal testing machine (Instron 5982, USA) with crosshead speed 1 mm/min and load cell 5 kN. During testing, certain amounts of load were applied on the sample until it fractured. Then, the value of compressive strength was calculated by dividing the load at fracture by cross-sectional area using the following expression:

$$\sigma = \frac{F_{\max}}{2(wt)} \quad (4)$$

where σ is compressive strength, $F_{\max}$ is the load applied during fracture and w and t is the width and thickness of the rectangular-shaped sample with dimensions, 15 mm × 15 mm × 15 mm.

3. Results and discussion

This work is focused on the porosity, cell skeleton, and strength of the sintered porcelain foam with respect to the different types of binder used. Fig. 1 shows the morphology of the polyurethane sponge used in this work. The sponge has a reticulated structure with connected open cells to allow fluid or slurry access and flow. The penetration of ceramic slurry into these channels during the replication process resulted in the coating of the sponge template. After the drying and sintering processes, the sponge was burnt out, leaving a structure of ceramic foam which retains the shape of the burned sponge. Therefore, the cell size of the porcelain foam fabricated depends on the sponge template used.

Thermal analysis was used to determine the burnout temperature of all the binders and sponge during the firing process. Based on the results, the optimum firing schedule used in the experimental section was determined. The thermal gravimetric analysis (TGA) thermo-gram for the binders and sponge are shown in Fig. 2. It is observed that the binders were decomposed in a three-step manner. The drying step and slow

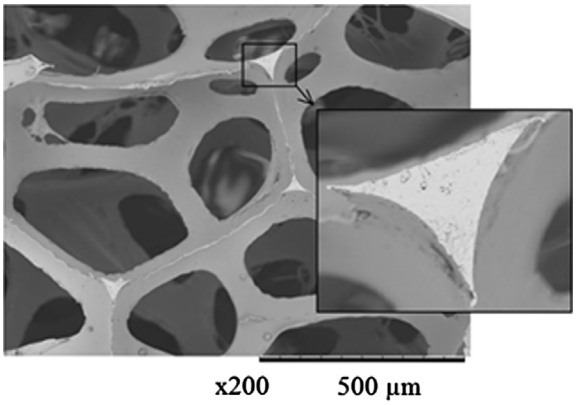

Fig.1. SEM image of the sponge used in this experiment. Inset show the triangular cross-sectional area of the sponge skeleton.

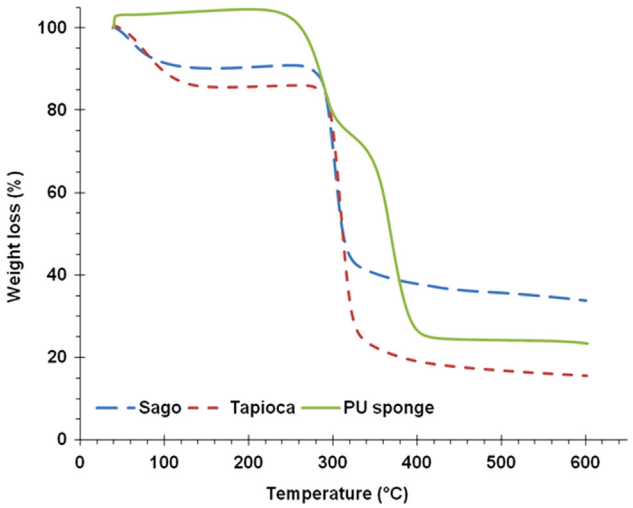

Fig. 2. TGA thermo-gram for the binders and sponge.

decomposition began at approximately 40 °C up to 130 °C, due to moisture evaporation and elimination of the crystallite phase (partially crystalline components; amylopectin molecules) for both, sago and tapioca starch. However, the excessive weight loss for sago and tapioca starch, shown by a steep decrease of the graph beginning approximately at 270–350 °C which is attributed to the decomposition of the starch leaving fraction of char residue and releasing masses of gaseous. At the end, there are small negligible weight reductions as the temperature passes 350 °C until the test was stopped. As for the sponge, there are no significant weight change was observed during the initial test. However, it started to decompose in a two-step manner with an obvious steep decrease at approximately 250–350 °C due to the decomposition of urethane bond; the second decrease happened between 350 °C and 420 °C attributed to loss of ester groups [27]. There is no further weight loss until the end of the test. For that, these results show that the soaking at 500 °C during the sintering process in order to eliminate the binders and sponge is suitable to use.

Sintered porcelain foam prepared in this experiment exhibited bulk density in the range of 0.375–0.744 g cm^{-3}, as shown in Fig. 3. According to the graph, the lowest density value of porcelain foam is shown by the samples with low solid loading (50 wt%), whilst the highest solid loading ratio (70 wt%) resulted in high density reading. The low density value shown by the sample with 50 wt% solid ratio can be associated to the low slurry density obtained because of less solid proportion was used. However, contrary to the samples with 70 wt% solid ratio, which had a high solid fraction, thus creating a higher density and a more viscous slurry, hence producing a high density porcelain foam in this case > 0.50 g cm^{-3} after sintered as previously stated by [7]. It has been observed that the density of porcelain foam is strongly influenced by the density of the slurry, as this also reflects the degree of viscosity.

The viscosity of the reference, sago and tapioca starch added slurries, measured at various shear rates are shown in Fig. 4.

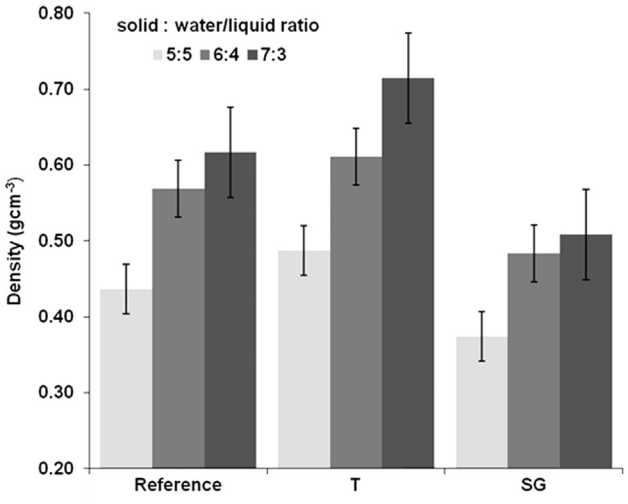

Fig. 3. Density of sintered porcelain foam varies with solid loading.

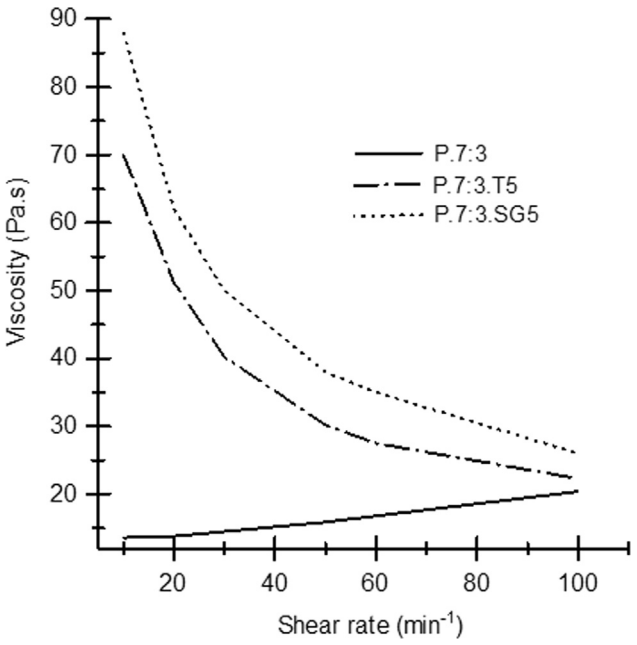

Fig. 4. Graph of viscosity versus shear rate for the slurries.

The slurries added with binder showed a pseudoplastic flow behavior. However, a Newtonian flow curve was shown by the reference slurry (P.7:3). Although the binder added slurries indicated a large difference in the viscosity compared to the reference at a lower shear rates, the viscosity values were not much different at higher shear rates. Since the slurries with binder behaved as pseudoplastic with low viscosity (14.9–26 Pa s) at high shear rates (> 80 min^{-1}), it was relatively easier to penetrate and fill the pores of the polymer sponge template during the replication process due to the ease of flow of the slurry. The thinning behavior of pseudoplastic slurry at high shear rate, caused the coated slurry on the template to become viscous once the removal of shear stress; subjected to compressed and release of sponge template during the fabrication process, thus making the coating thicker. The impregnation of the sponge template with these kinds of slurries results in the coating on the cell of the template. Besides that, due to the less fluid in the slurry and high contact of particles, an increase in solid content simultaneously lead to higher viscosity. Since the viscosity of the reference slurry is almost similar the other slurries at high shear rate, it will also produced a coated template after the impregnation process. The graph also reveals that P.7:3.SG5 has the highest viscosity reading amongst all of the slurries.

Fig. 5 shows the SEM micrographs of the broken skeleton from the porcelain foam structure after sintered. The cell sizes of the porcelain foam originated and depend on the sizes of original template used; therefore, they are open and linked together by solid skeletons replicating the template structure. The triangular voids at the interconnection of the skeletons are associated to the original skeleton of the sponge template (as shown in Fig. 1). The sponge template skeletons were burnout during sintering process, thus, it can be seen from Fig. 5 that the formation of coating with different thickness

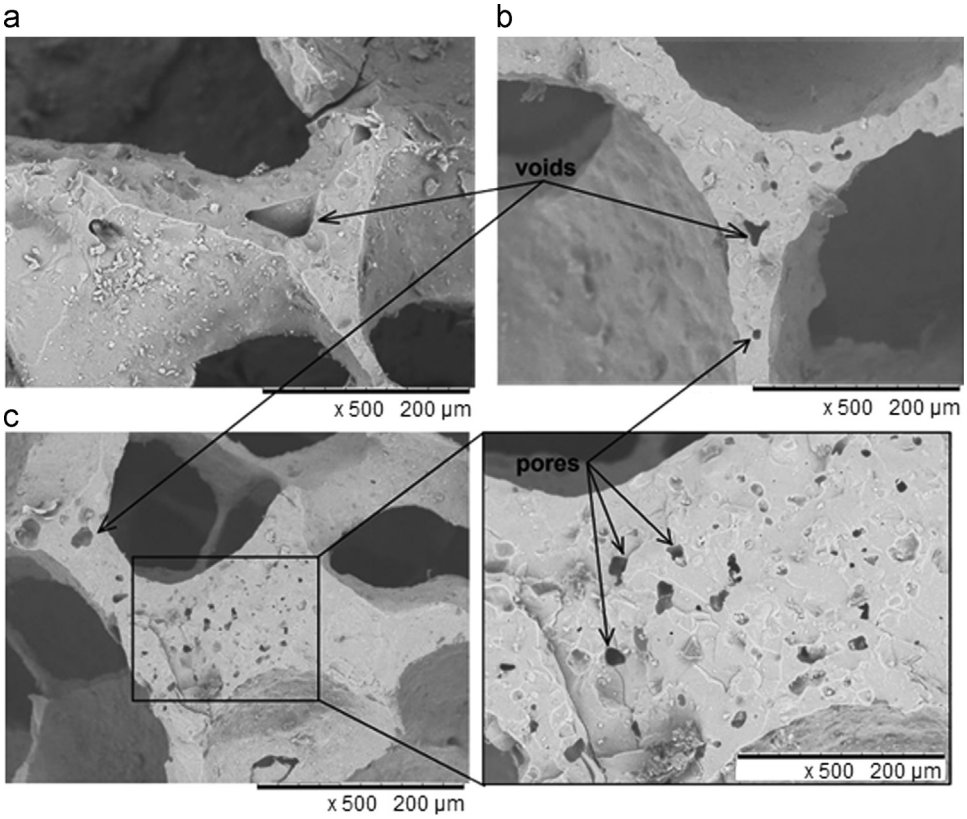

Fig. 5. SEM micrographs of voids and pores developed on the skeletons for the highest solid loading ratio samples: (a) P.7:3; (b) P.7:3.T5; and (c) P.7:3.SG5.

surrounding the voids. As stated earlier in the introduction, besides helping in the forming process and contributing to the green-body strength, the binders also act as a pore-forming agent. Porcelain foam without binder as in Fig. 5(a) only shows the existence of void. However, after binders were added into the slurry, the microscopic view on the rough surface of the skeletons showed an existence of a large number of fine pores with irregular shape and random distribution. The size of the pores appeared to be in micrometer range as seen in Fig. 5(b) and (c), respectively. Interestingly, the sample added with sago starch gave the most prominent number of pore development compared to the other type of binder.

The existence of these micro-size pores, mainly on samples added with sago can be associated to the low water content used for the slurry and fragments of sago generated during the mixing process as stated by Prabhakaran et al. [28] in the case of wheat particles. As the sago, which in agglomerated form added into the slurry, the moisture uptake by the sago starch granules is limited, so only part of the granule swells and turns into gel which later affects the rheological behavior of the slurry during mixing. Consequently, it had affecting the coating formation of slurry on the sponge template and green porosity. The unswelled fragments of sago starch granules stay as powder and later got burnt out during sintering, leaving pores on the skeletons. Maaruf et al. [25] explains this phenomenon by pointing out that, at high water levels, swelling of the starch granule causes the transformation of the crystallite region by pulling the crystallites apart

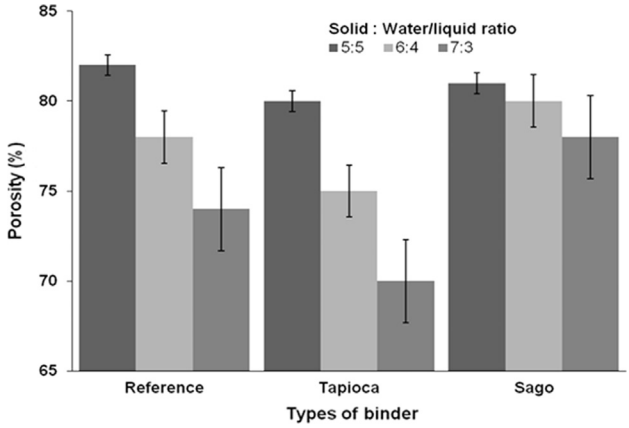

Fig. 6. The total porosity of porcelain foam varies with solid loading ratio and types of binder.

(the gelatinisation process), however, due to limited water presences, only part of the crystal structure will gelatinise leaving some granules only pre-swells or in their original form. As for the slurry added with tapioca starch, the fewer amount of pore developed can be associated due to the loose particle nature of the starch during the slurry processing, thus restricted the existence of tapioca fragments.

Fig. 6 shows the total porosity of the porcelain foam produced with various solid loadings and binders. Samples with low solid loading (darkest color) shows the highest percentage of porosity (greater than 80%). As seen from the

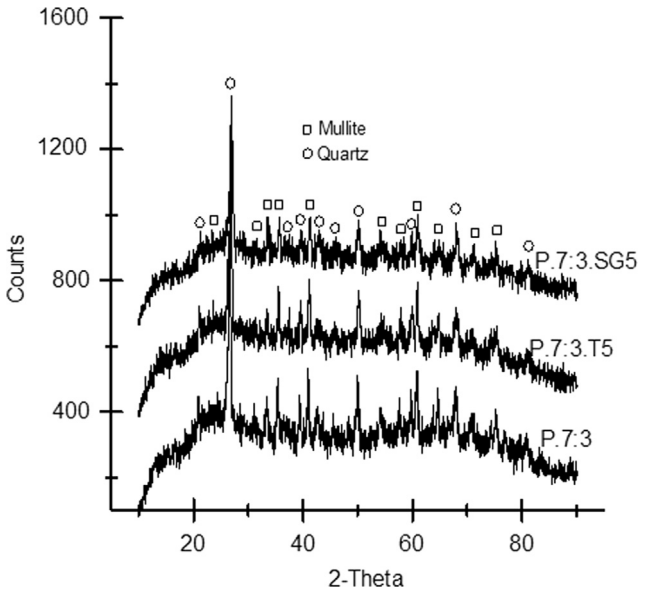

Fig. 7. XRD patterns of selected sintered samples.

figure, the percentage of porosity reduced as the solid loading of the samples increased. The reference and tapioca added samples show a significant porosity loss as the solid loading ratio increase to 60 wt%. However, the sample with sago starch addition has a quite constant porosity value (79–81%) even at different solid loadings.

The XRD patterns of samples with the highest solid loading ratio are shown in Fig. 7. The structure of the sintered porcelain foam is composed of crystalline and glassy phases. The identified crystalline structures consist of quartz (ICDD 00-046-1045) as the major phase, and mullite (ICDD 01-088-0890). Besides that, an amorphous glassy phase also exists within the samples as shown in the graph by a bulge distortion at 2-theta range between 15° and 35°. This glassy phase plays an important role in influencing the strength of the structure, since the silica network which exists within this region gives strength to the structure [29]. Furthermore, the region exists due to the richness of silica that was mainly contributed by the melting of feldspar component during the sintering process. Besides that, an abundant glassy phase is known to occur in porcelain wares.

The morphology of the sintered porcelain foams are shown in Fig. 8. The replication process of the polymer template creates open cell structure with inter-connected skeletons and channels forming high-porosity foam. All the sample have reticulated structure with cell size less than 1 mm. Fig. 8(a), (b) and (c), respectively, shows the microstructure of the open cells for the porcelain foam without binder addition. The cell skeletons in Fig. 8(a) are in poor and uneven condition with a few closed cells as compared to Fig. 8(b) and (c), respectively, which have a more uniform and increased number of closed cells. The case is quite similar with the other low solid loading compositions, even with binder additions as in Fig. 8(d), and (g), respectively. However, the surface of the skeleton became smoother and the amount of closed-cells are increasing as the solid loading increased to 60 wt% shown by Fig. 8(e) and (h), and 70 wt% of Fig. 8(f) and (i), respectively. Thus, samples with the highest solid loading ratio showed less number of fractured skeletons and better cell shapes. This is due to the thicker coating of slurry during the fabrication process which created a well-defined cell skeleton after sintered.

Fig. 9 illustrates the correlation of total porosity on the compressive strength of the samples at different solid loading and binders. The figure shows that the trend for all of the samples is quite similar. The enhanced compressive strength is shown by the higher solid loading samples, due to the lower porosity value. This result implies that the content of solid loading is disproportional of porosity but corresponding to strength. Besides that, it was also theoretically proven by Han et al. [30,31] that, after sintering, the percentage of porosity was reduced significantly that usually leads to higher strength. Brittle materials i.e., porcelain foam have demonstrated a relationship between the strength of porous material and the amount of porosity in the following expression [31,32]:

$$\sigma_{fc=}C\sigma_{fs}(1-P)^{3/2} \quad (5)$$

where σ_{fc} is the compressive strength of brittle foam in MPa, C is the geometric constant of the unit cell shape, σ_{fs} is the modulus of rupture of the cell-wall material, and P is the porosity value. Therefore, any changes in the porosity value i.e., the increase in porosity will result in the reduction of strength of the porous structure.

Earlier, it was stated that the amorphous or glassy phase has contributed to the strength of the structure. At the same time the compressive strength is also influenced by the formation of well-connected skeleton structure and cell size in the sintered porcelain foam. This can be seen in Fig. 8 with the presence of high number of intact skeletons in the foam network.

The skeletons structure also has sufficient thickness, less fracture and acceptable amount of closed cells. Besides that, with the increase of the cell uniformity and count of skeletons and junctions, the load reception and distribution in the porcelain foam structure increased during an application of loading. The graphs also suggest that the strength of all samples tallies with the percentage of porosity as stated in the theory. Sample P.7:3.SG5 gave an acceptable range of strength value with regards to the percentage of porosity obtained. This shows that the addition of sago starch as a binder in the porcelain foam is suitable for the production of porous structure.

4. Conclusions

Porcelain foams with the addition of various binders at different solid loading ratios have been successfully fabricated using the sponge replication technique. The density value for each sample was proportional to the solid loading ratio. The lowest solid loading ratio produced the highest porosity. Porcelain foam fabricated from slurry produced added with sago starch showed density, total porosity, and compressive strength of 0.37–0.51 g cm^{-3}, 79–81%, and 0.33–0.93 MPa, respectively. Samples added with sago starch also produced an

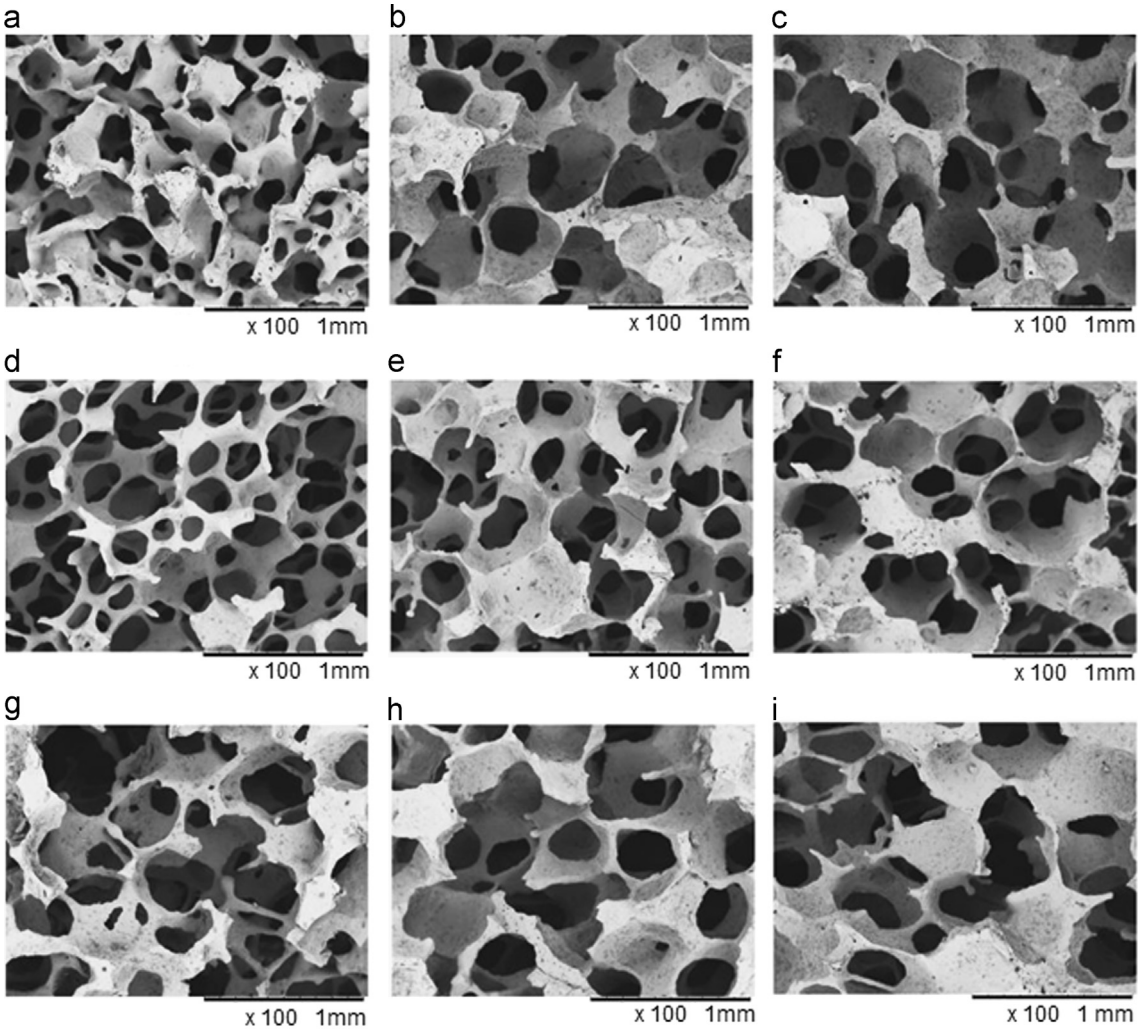

Fig. 8. SEM micrographs of porcelain foam produced with different solid loading and binder at 100 × magnification: (a) P.5:5; (b) P.6:4; (c) P.7:3; (d) P.5:5.T5; (e) P.6:4.T5; (f) P.7:3.T5; (g) P.5:5.SG5; (h) P.6:4.SG5; and (i) P.7:3.SG5.

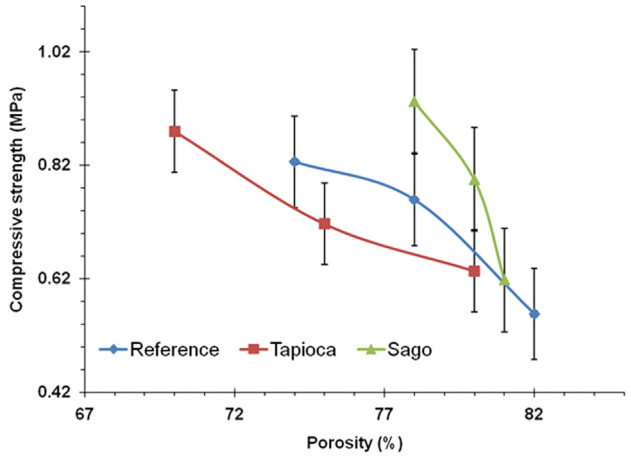

Fig. 9. The influence of porosity on the compressive strength with various solid loading and binder types.

almost similar porosity values for all different solid loadings. These acceptable compressive strength and porosity value derived from the slurry with sago starch are perhaps due to the addition of sago starch which resulted in higher value of viscosity and changes in the rheological property, consequently allowing the construction of smooth coating surface and less fractured skeleton although with the existence of micro-size pores after sintered.

Acknowledgments

The authors would like to acknowledge Universiti Sains Malaysia (USM) for funding this research under the RU-PRGS grant (1001/PBAHAN/8046032 and 1001/PMEKANIK/8044057).

References

[1] A. Julbe, D. Farrusseng, C. Guizard, Porous ceramic membranes for catalytic reactors—overview and new ideas, Journal of Membrane Science 181 (2001) 3–20.

[2] A.K. Ismail, M.Z. Abdullah, M. Zubair, Z.A. Ahmad, A.R. Jamaludin, K.F. Mustafa, M.N. Abdullah, Application of porous medium burner with micro-cogeneration system, Energy 50 (2013) 131–142.

[3] F. Cernuschi, S. Ahmaniemi, P. Vuoristo, T. Mantyla, Modelling of thermal conductivity of porous materials: application to thick thermal barrier coatings, Journal of the European Ceramic Society 24 (2004) 2657–2667.
[4] A. Mattern, B. Huchler, D. Staudenecker, R. Oberacker, A. Nagel, M.J. Hoffmann, Preparation of interpenetrating ceramic–metal composites, Journal of the European Ceramic Society 24 (2004) 3399–3408.
[5] K. Qiu, A. Hayden, Thermophotovoltaic power generation systems using natural gas-fired radiant burners, Solar Energy Materials and Solar Cells 91 (2007) 588–596.
[6] B.K. Nandi, R. Uppaluri, M.K. Purkait, Preparation and characterization of low cost ceramic membranes for micro-filtration applications, Applied Clay Science 42 (2008) 102–110.
[7] M. Muhamadnor, L. Hong, Z.A. Ahmad, H.M. Akil, Preparation and characterization of ceramic foam produced via polymeric foam replication method, Journal of Materials Processing Technology 207 (2008) 235–239.
[8] J. Garcia-ten, A. Saburit, E. Bernardo, P. Colombo, Development of lightweight porcelain stoneware tiles using foaming agents, Journal of the European Ceramic Society 32 (2012) 745–752.
[9] R.M. Khattab, M.M.S. Wahsh, N.M. Khalil, Preparation and characterization of porous alumina ceramics through starch consolidation casting technique, Ceramics International 38 (2012) 4723–4728.
[10] F. Yang, C. Li, Y. Lin, C. Wang, Effects of sintering temperature on properties of porous mullite/corundum ceramics, Materials Letters 73 (2012) 36–39.
[11] A. Dey, N. Kayal, O. Chakrabarti, Preparation of porous SiC ceramics by an infiltration technique, Ceramics International 37 (2011) 223–230.
[12] L.B. Garrido, M.P. Albano, K.P. Plucknett, L. Genova, Effect of starch filler content and sintering temperature on the processing of porous 3Y–ZrO_2 ceramics, Journal of Materials Processing Technology 209 (2009) 590–598.
[13] M.W. Quintero, J.A. Escobar, A. Rey, A. Sarmiento, C.R. Rambo, A.P.N. De Oliveira, D. Hotza, Flexible polyurethane foams as templates for cellular glass–ceramics, Journal of Materials Processing Technology 209 (2009) 5313–5318.
[14] H.D. Kim, T. Nakayama, B.J. Hong, K. Imaki, T. Yoshimura, T. Suzuki, H. Suematsu, K. Niihara, Fine-structured patterns of porous alumina material fabricated by a replication method, Journal of the European Ceramic Society 30 (2010) 2735–2739.
[15] L.J. Vandeperre, A.M. De Wilde, J. Luyten, Gelatin gelcasting of ceramic components, Journal of Materials Processing Technology 135 (2003) 312–316.
[16] L. Jing, K. Zuo, Z. Fuqiang, X. Chun, F. Yuanfei, The controllable microstructure of porous Al_2O_3 ceramics prepared via a novel freeze casting route, Ceramics International 36 (2010) 2499–2503.
[17] Y.W. Moon, K.H. Shin, Y.H. Koh, W.Y. Choi, H.E. Kim, Production of highly aligned porous alumina ceramics by extruding frozen alumina/camphene body, Journal of the European Ceramic Society 31 (2011) 1945–1950.
[18] R. Taktak, S. Baklouti, J. Bouaziz, Effect of binders on microstructural and mechanical properties of sintered alumina, Materials Characterizatio 62 (2011) 912–916.
[19] P. Colombo, Conventional and novel processing methods for cellular ceramics for cellular ceramics, Philosophical Transactions of the Royal Society A 364 (2006) 109–124.
[20] J.M. LeBeau, Y. Boonyongmaneerat, Comparison study of aqueous binder systems for slurry-based processing, Materials Science and Engineering: A 458 (2007) 17–24.
[21] E. Gregorova, W. Pabst, I. Boha, Characterization of different starch types for their application in ceramic processing, Journal of the European Ceramic Society 26 (2006) 1301–1309.
[22] M.H. Talou, M.A. Villar, M.A. Camerucci, Thermogelling behaviour of starches to be used in ceramic consolidation processes, Ceramics International 36 (2010) 1017–1026.
[23] E. Gregorova, W. Pabst, Z. Zivcova, I. Sedlarova, S. Holikova, Porous alumina ceramics prepared with wheat flour, Journal of the European Ceramic Society 30 (2010) 2871–2880.
[24] W. Pabst, E. Gregorova, Porous ceramics prepared using poppy seed as a pore-forming agent, Journal of the European Ceramic Society 33 (2007) 1385–1388.
[25] A.G. Maaruf, Y.B.C. Man, B.A. Asbi, A.H. Junainah, J.F. Kennedy, Effect of water content on the gelatinisation temperature of sago starch, Carbohydrate Polymers 46 (2001) 331–337.
[26] A.A. Karim, A.P. Tie, D.M.A. Manan, I.S.M. Zaidul, Starch from the sago (Metroxylon sagu) palm tree-properties, prospects, and challenges as a new industrial source for food and other uses, Comprehensive Reviews in Food Science and Food Safety 7 (2008) 215–228.
[27] G. Trovati, E.A. Sanches, S.C. Neto, Y.P. Mascarenhas, G.O. Chierice, Characterization of polyurethane resins by FTIR, TGA, and XRD, Journal of Applied Polymer Science 115 (2010) 263–268.
[28] K. Prabhakaran, A. Melkeri, N. Gokhale, S. Sharma, Preparation of macroporous alumina ceramics using wheat particles as gelling and pore forming agent, Ceramics International 33 (2007) 77–81.
[29] Y.S. Han, J.B.A.O. Li, B.O. Chi, Z.H.E. Wen, The effect of sintering temperature on porous silica composite strength, Journal of Porous Materials 10 (2003) 41–45.
[30] Y.S. Han, J.B. Li, Y.J. Chen, Fabrication of bimodal porous alumina ceramics, Materials Research Bulletin 38 (2003) 373–379.
[31] M.F. Ashby, R.E.M. Medalist, The mechanical properties of cellular solids, Metallurgical Transactions A 14 (1983) 1755–1769.
[32] X. Mao, S. Wang, S. Shimai, Porous ceramics with tri-modal pores prepared by foaming and starch consolidation, Ceramics International 34 (2008) 107–112.